HHS Public Access

Author manuscript

Ophthalmol Retina. Author manuscript; available in PMC 2024 August 01.

Published in final edited form as:

Ophthalmol Retina. 2023 August ; 7(8): 672–682. doi:10.1016/j.oret.2023.03.016.

Symmetry of Macular Fundus Features in Age-Related Macular Degeneration

Omer Trivizki, MD, MBA[1,2], **Liang Wang, Bsc.**[1], **Yingying Shi., MD**[1], **David Rabinovitch, Bsc**[2], **Prashanth Iyer, MD**[1], **Giovanni Gregori, PhD**[1], **William Feuer, Ms**[1], **Philip J. Rosenfeld, MD, PhD**[1]

[1]Department of Ophthalmology, Bascom Palmer Eye Institute, University of Miami Miller School of Medicine, Miami, Florida.

[2]Department of Ophthalmology, Tel Aviv Medical Center, University of Tel Aviv, Tel Aviv, Israel

Abstract

PURPOSE—The symmetry of major macular fundus features in both eyes of the same patient with age-related macular degeneration (AMD) was investigated using swept-source optical coherence tomography (SS-OCT).

DESIGN: Retrospective review of a prospective study

PARTICIPANTS: Patients with AMD

METHODS—Grading was performed on the first SS-OCT images obtained on the patients. Two graders diagnosed the presence of drusen, geographic atrophy (GA), and exudative AMD (eAMD) in each eye. Medical records were reviewed to assess prior exudation. To assess symmetry, one eye of each patient was randomly selected as the index eye and compared with the fellow eye. The kappa statistic (κ) was used to assess symmetry of diagnosis. The intraclass correlation coefficient (ICC) was used to assess the symmetry of drusen area and volume.

Main Outcome Measured: interocular symmetry of AMD stages: drusen, GA and eAMD.

RESULTS—A total of 1310 patients with AMD were included. The average age was 78 years old (range, 50–102; 60% women). Of the 1310 subjects, 54% (701) presented with symmetric disease; 20% with bilateral drusen, 11% with bilateral GA, and 22% with bilateral eAMD. Only 0.5% of subjects had both GA and eAMD in both eyes. Of the randomly selected index eyes, 825 (47%) were right eyes. Overall, limited interocular agreement was observed between index and fellow eyes (54%; $\kappa = 0.29$). Kappa coefficients were poor (<0.4) for index eyes diagnosed with drusen ($\kappa = 0.27$), eAMD ($\kappa = 0.17$), and mixed disease ($\kappa = 0.03$). There was moderate agreement

Corresponding Author: Philip J. Rosenfeld MD, PhD, Bascom Palmer Eye Institute, 900 NW 17th street, Miami, FL, 33136, Voice: 305-326-6148, prosenfeld@miami.edu.

DISCLOSURES:

b.Financial Disclosures:
The remaining authors have no disclosures.

between index and fellow eyes for GA (κ = 0.50). Of the 265 patients with bilateral drusen, the symmetry of drusen area measurements had moderate ICC values of 0.70, 0.71, and 0.70 in the 3mm and 5mm diameter foveal-centered circles and in the total scan area, respectively. The ICC values for the drusen volumes were 0.65, 0.66, and 0.64 respectively.

CONCLUSION—Interocular symmetry was poor for eyes with drusen, eAMD, and mixed disease, but moderate for GA. While the diagnosis of drusen was not very symmetric between eyes, when present in both eyes, the drusen area and volume measurements were moderately symmetric.

PRECIS

AMD patients showed poor interocular symmetry for drusen, exudative AMD, and mixed disease, but moderate symmetry for GA patients. The area and volume measurements of drusen were moderately symmetric in patients with bilateral drusen.

Keywords

Age-related macular degeneration; Swept-source OCT; Symmetry; Drusen area; Drusen Volume; Geographic atrophy; Macular neovascularization

INTRODUCTION

Age-related macular degeneration (AMD) is the leading cause of irreversible vision loss among the elderly worldwide and involves the complex interaction of both genetic and environmental factors.[1] AMD is characterized by drusen, which histopathologically corresponds to the accumulation of extracellular lipids and protein under the retinal pigment epithelium (RPE) monolayer resulting in focal elevations between the RPE and Bruch's membrane (BM). With disease progression, there is migration of RPE cells into the retina, which appear as pigment clumps on color fundus imaging and slit-lamp biomicroscopy, and as hyper-reflective foci on OCT imaging.[2,3] The loss of the RPE along with the loss of photoreceptors and the choriocapillaris are characteristic features of geographic atrophy (GA), a late stage of AMD also known as complete RPE and outer retinal atrophy (cRORA).[4,5] With disease progression, another possible outcome is the formation of non-exudative and exudative macular neovascularization (MNV)[6–8]

Clinically, the stages of AMD are classified using color fundus imaging and fundus examination into three stages; early, intermediate, and late.[4] Early and intermediate AMD are distinguished based on the size of macular drusen and the presence of pigment, while the late stages are diagnosed based on the presence of GA (cRORA), exudative MNV, or both. AMD has a genetic basis, but environmental factors such as smoking, poor nutrition, obesity, diabetes, hypertension, and cardiovascular disease are also expected to influence its progression. [9,10] Despite expectations that similar environmental exposures in both eyes should lead to similar disease stages, it is noteworthy that earlier stages of AMD tend to present with high concordance, and this concordance decreases as the disease progresses. [11] Eventually, as the disease progresses to its end-stage, the advanced late-stage of AMD becomes more symmetric.[12–15] One possible explanation for this discordance of disease

progression is that genetics plays a significant role in disease onset and early progression, while the impact of environmental influences may fluctuate over time with a variable impact on disease progression in each eye. How these environmental influences impact one eye more than the other remains an unanswered and provocative observation. Eventually, if the patient lives long enough, both eyes achieve the end-stage of disciform scars or macular atrophy.

To confirm and better understand the extent of symmetry in the stage of disease between eyes, we performed a cross-sectional study to characterize disease severity in both eyes using swept-source optical coherence tomography (SS-OCT). Unlike previous studies exploring AMD symmetry, which were based predominantly on color fundus imaging, this study analyzed quantitative SS-OCT characteristics not previously described in the literature for this purpose. [1,11,12,16] We did not use the early and intermediate AMD categories because color fundus images were not available for all patients on SS-OCT imaging dates. Instead, we classified the eyes with AMD into OCT anatomic categories such as drusen, GA, and current or prior exudation.

MATERIAL AND METHODS

Patients with AMD were enrolled in a prospective SS-OCT observational study at the Bascom Palmer Eye Institute. The Institutional Review Board of the University of Miami Miller School of Medicine approved this study, and all patients signed the informed consent. The study was performed in accordance with the tenets of the Declaration of Helsinki and complied with the Health Insurance Portability and Accountability Act of 1996.

Imaging Protocol

For this current report, a retrospective review was performed of all AMD patients prospectively enrolled from April 2016, when the latest version of the SS-OCT instrument was delivered, to June 2021. This is the first study ever to address the symmetry question using a quantitative OCT method. Previous studies were based on color fundus imaging. To be included in this study, subjects had to be over the age of 50. SS-OCT (PLEX Elite 9000, Carl Zeiss Meditec, Dublin, CA) images were obtained using an SS-OCT-A instrument with a scanning rate of 100,000 A-scans per second that had a swept-source laser with a central wavelength of 1,060 nm, resulting in full width at half maximum axial resolution of 5.0 microns in tissue and a lateral resolution of 20 microns estimated at the retinal surface. One 6×6 mm volume scan centered on the fovea was selected for each eye at their first visit. Only scans with a signal strength of 7 or greater without motion artifacts were retained. Each 6×6 mm scan consists of 500 A-scans and 500 B-scans. Each B scan was repeated twice at the same position, resulting in a homogenous sampling grid with a separation of 12 microns.

For each patient, the scans from their first imaging session were considered for the purposes of this paper. Patients were allowed to be on active anti-VEGF treatment. Exclusion criteria included any prior vitreoretinal surgery or any other retinal disease that would affect the retina, such as diabetic retinopathy, retinal vein occlusion, central serous chorioretinopathy, and pathologic myopia. In addition, demographic information was obtained by performing a retrospective chart review.

Swept-Source OCT Image Processing

Two independent investigators performed grading for the presence of drusen, GA (cRORA), and exudative AMD using SS-OCT structural and angiographic images (OT, LW). Graders tried to reach a consensus and when needed, a senior grader (PJR) adjudicated any disagreements. In addition, the diagnosis of previous or current exudative MNV was determined by reviewing the medical records and by reviewing the SS-OCT angiographic scans. GA, also referred to as cRORA, was identified by detecting persistent choroidal hypertransmission defects on en face SS-OCT images along with individual B-scans as previously described. Typical drusen that resulted in an elevation of the RPE were measured.[17, 18]SS-OCT validated software automatically determined the area and volume of drusen within the foveal-centered circles with diameters of 3 mm and 5 mm, as well as within the total scan area.[19] A square-root transformation was applied for the analysis of drusen area measurements, and a cube-root transformation was applied for the analysis of drusen volumes since these transformations decreased the influence of drusen size and volume on the test-retest variability.[20] To assess the magnitude of intraocular differences (IODs) in drusen area and volume measurements, a randomly selected eye for each patient was identified as an index eye, and then the fellow eye was compared to the index eye. For the analysis of GA, *en face* images were generated from all 6X6 mm scans. The *en face* images were created using a sub-RPE slab positioned 64 to 400μm beneath Bruch's membrane as previously reported,[3,21–23] and these images are highly correlated with the areas of GA measured using autofluorescence [24,25] All en face images were graded for the presence of persistent choroidal hypertransmission defects or cRORA. On the *en face* images, GA was identified as an area of increased focal brightness corresponding to the hypertransmission of light into the choroid measuring at least 250μm in greatest linear dimension.[3,21–23]These areas are also known as persistent choroidal hypertransmission defects (hyperTDs). Measurements of the GA area were not performed since the 6X6mm scan can be used to detect for the presence of GA, but the GA could extend beyond the 6×6 mm FOV of the scan. Therefore, accurate measurements and comparisons of total GA lesion area were not always possible. In addition, fundus autofluorescence images were not routinely obtained on these eyes with AMD.

Statistical Analyses

Statistical analyses were performed using SPSS 27.0 (IBM Statistical Package for Scientific Studies for Windows, Armonk NY). The between eye agreement of AMD gradings was summarized using interocular observed agreement and Cohen's kappa Coefficient [26] (k<0.4, poor agreement; k:0.4 to 0.75, fair to good agreement; k>0.75, excellent agreement). Between eye agreement of drusen areas and volumes were assessed with the intraclass correlation (ICC). [27,28] Linear regression and Pearson's r^2 were used to study the association between interocular differences and drusen area and volume. P values of less than 0.05 were considered to be statically significant.

RESULTS

A total of 1850 AMD patients were reviewed, and 1310 met the criteria for inclusion in this study. All subjects had evidence of bilateral disease. The average age of the 1310 patients

in the study was 78 (range, 50–102) and 60% were women. We considered the following categories of disease: drusen only, GA, exudative MNV (eAMD), and eyes with mixed disease (i.e., both GA and eAMD) as shown in Figures 1–5. The last three categories are considered a late-stage disease.

Overall Symmetry Between Eyes

Table 1 shows the percentage agreement of disease gradings between the two eyes, and neither eye showed a predilection for a particular stage of disease. There was an overall observed interocular agreement of 54% ($\kappa = 0.29$). The relatively low Cohen kappa value indicates that AMD is a disease with poor symmetry based on our staging of the disease as drusen-only eyes versus late-stage eyes. The late stage is further divided into GA and eAMD. Table 1 shows that 54% of the patients (701) presented with symmetric disease gradings; of these 20% had bilateral drusen, 11% had bilateral GA, and 22% had bilateral exudative MNV (eAMD). Only 1% of patients had both GA and eMNV co-occurring in both eyes. Kappa coefficients were poor (<0.4) for index eyes diagnosed with drusen (κ =0.27), eAMD ($\kappa = 0.17$), and mixed disease ($\kappa = 0.03$). There was moderate agreement between index and fellow eyes for GA ($\kappa = 0.50$).

Symmetry Between Eyes with Drusen

The subgroup of patients with bilateral drusen was analyzed further. A total of 265 patients were identified with only drusen in both eyes. This group's average age was 73.4 (51–93), with 63% women. Figure 6 shows scatter plot comparisons of drusen area and volume measurements within the foveal-centered circles with diameters of 3 mm and 5 mm, as well as within the total scan area (all p>0.07). Table 2 characterizes the percentage of interocular differences (right eye minus the left eye) for drusen area and volume measurements for 50% and 95% of the distributions. When symmetry was assessed using the square-root drusen area measurements for patients with bilateral drusen, moderate ICC values of 0.70, 0.71, and 0.70 for the 3 mm circle, 5 mm circle, and the total scan area, respectively, indicating good agreement. The ICC for cube-root drusen volume was slightly lower with 0.65, 0.66, and 0.64, respectively. Figure 7 shows the scatter plot correlations between the square-root of drusen area and the cube-root of drusen measurements versus their intraocular differences. When trying to fit the data using linear, quadratic, cubic, growth, or exponential tests, we found no association using any of the tests performed with all r-squared values less than 0.03 (3%). However, when drusen square-root areas and cube-root volumes were divided into quintiles, the smallest quintile had the smallest interocular differences (table 3).

DISCUSSION

Since AMD is a genetic disease with environmental influences, we might have expected a higher degree of symmetry between eyes since both genetics and most environmental influences would be expected to be the same in both eyes. Our earlier expectations were reinforced by studies which reported higher rates of symmetry across all stages of the disease. Using the Minnesota Grading System (MGS) based on AREDS, overall symmetry has been reported to be as high as 95% in small datasets (n=20), [16] which is strikingly dissimilar to the 54% symmetry and low interocular agreement (k<0.4) found in our study

(n=1310). One possible explanation for their findings is that they were grading eye bank eyes, which were likely to have more advanced stages of AMD. We used a broad 3-step staging system that classified eyes into a drusen-only stage and a late stage of AMD, with the late-stage further divided into GA and eAMD, and only requirement that we had for imaging was that the patient had a diagnosis of AMD and was seen at the Bascom Palmer Eye Institute.[29] Moreover, our SS-OCT staging system is a minor modification of the classification system based on color fundus imaging and should be comparable in identifying eyes at risk for progression since we provide a detailed quantitative assessment of drusen area and volume, which we have shown are predictive of disease progression from intermediate to late AMD.[4,20,23] Since the stage of intermediate AMD depends on drusen size, we believe that our staging system might be even more representative of disease progression and better than color fundus imaging for assessing the symmetry of disease between eyes. The applicability of our staging system based on SS-OCT imaging is supported by studies which have shown similar rates of AMD bilaterality to the present study. For example, Pai et al. reported bilateral disease in 60.4% of patients with any stage of disease based off photographic grading using the Wisconsin system, whereas 54% of our patients had bilateral disease.[30]

Compared with a study of 81 patients with bilateral drusen which reported good to excellent symmetry of several drusen characteristics,[31] we found limited interocular agreement ($k<0.4$) across the 265 patients with bilateral drusen, with the smallest difference in the drusen measurements found in the smallest quintile for drusen area and drusen volume. It is interesting to note that a large druse, which has a diameter of 125μm on color fundus imaging and is sufficient to define an eye as having intermediate AMD (iAMD)[4] would have a square-root area of about 0.11 μm. Figure 6 demonstrates that the vast majority of the drusen eyes included in this study have a total drusen volume that far exceeds the color fundus grading for large drusen and iAMD. This suggests that there's more symmetry at the stage of AMD consistent with iAMD on color fundus imaging with drusen asymmetry becoming more prevalent as the disease progresses and the drusen burden increases.

Since drusen area and volume measurements have been shown to correlate with the complement factor H at-risk allelic burden in patients with AMD,[32–38] it would appear that genetics and environmental influences that are shared between eyes play an essential role at this early drusen stage, but once the drusen volume and area enlarge and the eye with drusen progresses to the late stage of AMD, this early-onset symmetry is lost. These drusen results resemble previous data evaluating phenotypic symmetry in monozygotic twins, which showed moderate symmetry between twins for the occurrence of soft and hard drusen, with symmetry of 57% and 80%, respectively.[39] In this previous twin study, drusen were evaluated using stereoscopic macular photographs rather than a more quantitative imaging technology such as SS-OCT, which we believe is a better approach for quantifying the symmetry of drusen between eyes. By using SS-OCT imaging, we refined the quantifiable grading of drusen area and volume measurements in both eyes to show an ICC of 0.6–0.7.

Since we were looking at a cross-section of disease progression with a common end-stage of AMD being the formation of GA and eAMD, which are often associated with the loss of visual function and the reason why most patients seek out a retina specialist, we expected to

find that GA and eAMD would be symmetric between eyes since they represent a common endpoint of disease progression and they are associated with loss of visual function.[11] This has been shown in previous studies evaluating patients with GA[12,40] disciform scars [13,15] However, we were surprised to find that only 11% of patients had bilateral GA and 22% had bilateral exudative MNV (eAMD), with only 1% of patients having both GA and eMNV co-existing in both eyes. While we expected the best kappa coefficient to be found for index eyes with GA, since GA does represent the end-stage of non-exudative AMD and it's the most common form of late AMD, only a moderate agreement between index and fellow eyes with GA ($\kappa = 0.50$) was found. In contrast, for eyes with eAMD, another common disease endpoint, the kappa was poor ($\kappa = 0.17$) and even worse for mixed disease ($\kappa = 0.03$). This contributes to the relatively low overall kappa of 0.29 indicating poor symmetry overall when including both drusen-only eyes and late-stage AMD eyes. One possible explanation for the low symmetry of advanced end-stage disease in our study is that these patients may not seek out the inconvenience of tertiary specialty care given their extensive vision loss, and another explanation might be a selection bias in excluding patients with advanced end-stage disease to undergo SS-OCT imaging with the realization that central fixation and image quality would prevent the acquisition of useful images and that their imaging at follow-up visits would not be particularly informative about disease progression even if they decided to return.

For bilateral eyes with GA, a comparison of GA area measurements between eyes would have been ideal, but due to the FOV limitations of our 6X6 mm scan pattern, we could not fully quantify the larger areas of GA that exceeded the scan's FOV; however, this SS-OCT scan pattern was able to easily identify whether any macular GA related to AMD within the arcades was present, it was just the extent of atrophy that could not be fully quantified. Another feature related to bilateral GA is whether the GA was foveal or non-foveal, but that assessment was not undertaken since the outcome would not have impacted the clinical stage of AMD and the question of foveal involvement deals more with the symmetry of disease onset and progression, which is the focus of ongoing longitudinal studies. Despite these limitations, we did observe moderate agreement between eyes with the diagnosis of any macular GA. At least, we can conclude that GA subjects were found to have a more symmetric disease than other stages ($\kappa = 0.50$), with slightly more than 10% showing GA in both eyes at the time of their first scan.

Regarding the symmetry of eAMD, 815 patients had eAMD in at least one eye, and 35% of these patients had bilateral exudative disease with poor concordance between the eyes of the same patients. These results are consistent with previously published data indicating relatively lower levels of symmetry in eAMD.[11] Multiple studies suggest that exudative disease in one eye significantly increases the risk of conversion to exudative disease in the fellow eye, implying that greater symmetry should be present if all these patients had been followed longer.[41–43] Strahlman *et al.*[43] conducted a retrospective study on 84 patients with unilateral eAMD in one eye and only drusen in the other eye. For the three years following the initial presentation, they reported a three to seven percent annual risk of developing eAMD in the second eye. This was confirmed by the AREDS data that suggested a 10% per year risk of developing an exudative disease in the fellow eye with an overall risk of about 50% at five years.[29] These studies show a tendency to progress to symmetrical eAMD,

which was not captured by our cross-sectional study that provides only a snapshot in time. While the asymmetry that we detected between eyes in the late stage of AMD may simply reflect a random stochastic process, it is also possible that there could be an underlying asymmetry with respect to environmental factors that are different between eyes, which then might influence disease progression differently between the two eyes. One possible environmental influence is the difference in the ocular perfusion between eyes.[44,45]

Limitations of this study include its cross-sectional nature with patients seen at a tertiary care referral retina clinic for AMD, and these patients would likely be symptomatic and more advanced at the time of presentation. However, even with this limitation, a range of disease severities was observed. Another limitation was the use of SS-OCT imaging with a 6X6 mm FOV since GA and MNV could appear and extend beyond this FOV. While CF and FAF imaging were obtained on some of the patients, all the patients in this study received SS-OCT imaging. While it is theoretically possible that both GA and exudative MNV could develop outside the 6X6 FOV in AMD, it is highly unlikely based on clinical experience and current scanning protocols used in clinical trials. Moreover, the FOV was used to assess whether GA or MNV were present and not to determine the full extent of the lesions or the growth rates of the lesions. Using 12X12mm scans that were obtained on most patients, we should be able to address the symmetry of GA size in future investigations.

Our study highlights the potential impact of non-genetic factors on disease progression and the importance of assessing both eyes separately in the diagnosis and management of AMD. While drusen area and volume appear to be strongly influenced by genetics and serve as important diagnostic criteria for AMD, the asymmetry beyond the early drusen stage most likely involves more than just genetics, with the likely candidates being environmental factors that may asymmetrically impact disease progression between eyes. Such environmental factors would be ideal candidates for targeted interventions that may slow overall disease progression. While it could be argued that the population included in this study represents patients who are being seen in a referral retina practice with more advanced disease and are not representative of the entire spectrum of AMD, it is noteworthy that we did have a patient population with small drusen and it was this smallest quintile that showed the highest degree of symmetry. One interesting additional finding from this study was the lack of phenotypic preference for either eye determined by random indexing, allowing future studies to further investigate AMD symmetry without concern of a bias between eyes.

By better understanding how environmental factors influence macular health and how these factors may differ between the eyes of the same patient, we can gain new insights into how the development of future targeted therapies may slow disease progression. Our findings have important implications for the development of these targeted therapies, such as therapies designed to improve ocular perfusion. These therapies might be tailored to the specific eye with more advanced asymmetric disease, thus potentially improving the clinical care of patients with AMD.

Funding/Support:

Research supported by grants from Carl Zeiss Meditec, Inc., the Salah Foundation, an unrestricted grant from the Research to Prevent Blindness, Inc. (New York, NY), and the National Eye Institute Center Core Grant (P30EY014801) to the Department of Ophthalmology, University of Miami Miller School of Medicine. The funding organizations had no role in the design or conduct of the present research.

Giovanni Gregori and Philip J. Rosenfeld received research support from Carl Zeiss Meditec, Inc. Giovanni Gregori and the University of Miami co-own a patent that is licensed to Carl Zeiss Meditec, Inc. Dr. Rosenfeld also received research funding from Gyroscope Therapeutics and Stealth BioTherapeutics. He is also a consultant for Apellis, Boehringer-Ingelheim, Carl Zeiss Meditec, Chengdu Kanghong Biotech, InflammX Therapeutics, Ocudyne, Regeneron Pharmaceuticals, and Unity Biotechnology. He also has equity interest in Apellis, Valitor, Verana Health, and Ocudyne.

Abbreviations and Acronyms

AMD	Age-related Macular Degeneration
SS-OCT	Swept-Source Optical Coherence Tomography
GA	Geographic Atrophy
MNV	macular neovascularization

References

1. Fleckenstein M, Keenan TDL, Guymer RH, et al. Age-related macular degeneration. Nat Rev Dis Primers. May 6 2021;7(1):31. doi:10.1038/s41572-021-00265-2 [PubMed: 33958600]
2. Cao D, Leong B, Messinger JD, et al. Hyperreflective Foci, Optical Coherence Tomography Progression Indicators in Age-Related Macular Degeneration, Include Transdifferentiated Retinal Pigment Epithelium. Invest Ophthalmol Vis Sci. Aug 2 2021;62(10):34. doi:10.1167/iovs.62.10.34
3. Laiginhas R, Shi Y, Shen M, et al. Persistent Hypertransmission Defects Detected on En Face Swept Source Optical Computed Tomography Images Predict the Formation of Geographic Atrophy in Age-Related Macular Degeneration. Am J Ophthalmol. May 2022;237:58–70. doi:10.1016/j.ajo.2021.11.001 [PubMed: 34785169]
4. Ferris FL 3rd, Wilkinson CP, Bird A, et al. Clinical classification of age-related macular degeneration. Ophthalmology. Apr 2013;120(4):844–51. doi:10.1016/j.ophtha.2012.10.036 [PubMed: 23332590]
5. Sadda SR, Guymer R, Holz FG, et al. Consensus Definition for Atrophy Associated with Age-Related Macular Degeneration on OCT: Classification of Atrophy Report 3. Ophthalmology. Apr 2018;125(4):537–548. doi:10.1016/j.ophtha.2017.09.028 [PubMed: 29103793]
6. Shen M, Rosenfeld PJ, Gregori G, Wang RK. Predicting the Onset of Exudation in Treatment-Naive Eyes with Nonexudative Age-Related Macular Degeneration. Ophthalmol Retina. Jan 2022;6(1):1–3. doi:10.1016/j.oret.2021.10.006 [PubMed: 34996537]
7. Spaide RF, Jaffe GJ, Sarraf D, et al. Consensus Nomenclature for Reporting Neovascular Age-Related Macular Degeneration Data: Consensus on Neovascular Age-Related Macular Degeneration Nomenclature Study Group. Ophthalmology. May 2020;127(5):616–636. doi:10.1016/j.ophtha.2019.11.004 [PubMed: 31864668]
8. Yang L, Meng H, Luo D, et al. Inhibition of Experimental Age-Related Macular Degeneration by ZQMT in Mice. Curr Mol Med. 2019. 434–442:)6(19; doi:10.2174/1566524019666190425195706 [PubMed: 31288713]
9. Lambert NG, ElShelmani H, Singh MK, et al. Risk factors and biomarkers of age-related macular degeneration. Prog Retin Eye Res. Sep 2016;54:64–102. doi:10.1016/j.preteyeres.2016.04.003/10.1016j.preteyeres.2016.04.003. Epub 2016 May 6. [PubMed: 27156982]

10. Ammar MJ, Hsu J, Chiang A, Ho AC, Regillo CD. Age-related macular degeneration therapy: a review. Curr Opin Ophthalmol. May 2020;31(3):215–221. doi:10.1097/ICU.0000000000000657 [PubMed: 32205470]
11. Mann SS, Rutishauser-Arnold Y, Peto T, et al. The symmetry of phenotype between eyes of patients with early and late bilateral age-related macular degeneration (AMD). Graefes Arch Clin Exp Ophthalmol. Feb 2011;249(2):209–14. doi:10.1007/s00417-010-1483-x/10.1007s00417-010-1483-x. Epub 2010 Aug 25. [PubMed: 20737163]
12. Bellmann C, Jorzik J, Spital G, Unnebrink K, Pauleikhoff D, Holz FG. Symmetry of bilateral lesions in geographic atrophy in patients with age-related macular degeneration. Archives of ophthalmology (Chicago, Ill : 1960). May 2002;120(5):5. 79–84 doi:10.1001/archopht.120.5.579/10.1001archopht.120.5.579.
13. Dow ER, Adeghate JO, Coombs PG, Gupta Patel M, D'Amico DJ, Kiss S. Fellow-Eye Conversion and Treatment in Exudative Age-Related Macular Degeneration. Journal of VitreoRetinal Diseases. 438–444:)6(3;2019. doi:10.1177/2474126419865990
14. Fleckenstein M, Adrion C, Schmitz-Valckenberg S, et al. Concordance of disease progression in bilateral geographic atrophy due to AMD. Invest Ophthalmol Vis Sci. Feb 2010;51(2):637–42. doi:10.1167/iovs.09-3547/10.1167iovs.09-3547. Epub 2009 Sep 24. [PubMed: 19797219]
15. Lavin MJ, Eldem B, Gregor ZJ. Symmetry of disciform scars in bilateral age-related macular degeneration. Br J Ophthalmol. Mar 1991;75(3):133–6. doi:10.1136/bjo.75.3.133/10.1136bjo.75.3.133. [PubMed: 1707308]
16. Olsen TW, Feng X. The Minnesota Grading System of Eye Bank Eyes for Age-Related Macular Degeneration. Investigative Ophthalmology & Visual Science. 2004;45(12):4484–4490. doi:10.1167/iovs.04-0342 [PubMed: 15557458]
17. Laiginhas R, Shi Y, Shen M, et al. Persistent Hypertransmission Defects Detected on En Face Swept Source Optical Computed Tomography Images Predict the Formation of Geographic Atrophy in Age-Related Macular Degeneration. American Journal of Ophthalmology. 2022/05/01/2022;237:58–70. doi:10.1016/j.ajo.2021.11.001 [PubMed: 34785169]
18. Liu J, Laiginhas R, Corvi F, et al. Diagnosing Persistent Hypertransmission Defects on En Face OCT Imaging of Age-Related Macular Degeneration. Ophthalmology Retina. 2022/05/01/2022;6(5):387–397. doi:10.1016/j.oret.2022.01011. [PubMed: 35093585]
19. Jiang X, Shen M, Wang L, et al. Validation of a Novel Automated Algorithm to Measure Drusen Volume and Area Using Swept Source Optical Coherence Tomography Angiography. Transl Vis Sci Technol. Apr 1 2021;10(4):11. doi:10.1167/tvst.10.4.11
20. Gregori G, Wang F, Rosenfeld PJ, et al. Spectral domain optical coherence tomography imaging of drusen in nonexudative age-related macular degeneration. Ophthalmology. Jul 2011;118(7):1373–9. doi:10.1016/j.ophtha.2010.11.013
21. Liu Y, Holekamp NM, Heier JS. Prospective, Longitudinal Study: Daily Self-Imaging with Home OCT for Neovascular Age-Related Macular Degeneration. Ophthalmol Retina. Feb 28 2022;doi:10.1016/j.oret.2022.02.011
22. Shi Y, Zhang Q, Zhou H, et al. Correlations Between Choriocapillaris and Choroidal Measurements and the Growth of Geographic Atrophy Using Swept Source OCT Imaging. Am J Ophthalmol. Apr 2021;224:321–331. doi:10.1016/j.ajo.2020.12.015 [PubMed: 33359715]
23. Schaal KB, Rosenfeld PJ, Gregori G, Yehoshua Z, Feuer WJ. Anatomic Clinical Trial Endpoints for Nonexudative Age-Related Macular Degeneration. Ophthalmology. May 2016;123(5):1060–79. doi:10.1016/j.ophtha.2016.01.034
24. Velaga SB, Nittala MG, Hariri A, Sadda SR. Correlation between Fundus Autofluorescence and En Face OCT Measurements of Geographic Atrophy. Ophthalmol Retina. Aug 2022;6(8):676–683. doi:10.1016/j.oret.2022.03.017 [PubMed: 35338026]
25. Yehoshua Z, Garcia Filho CA, Penha FM, et al. Comparison of geographic atrophy measurements from the OCT fundus image and the sub-RPE slab image. Ophthalmic surgery, lasers & imaging retina. Mar-Apr 2013;44(2):127–32. doi:10.3928/23258160-20130313-05
26. Maguire MG. Assessing Intereye Symmetry and Its Implications for Study Design. Invest Ophthalmol Vis Sci. Jun 3 2020;61(6):27. doi:10.1167/iovs.61.6.27

27. Gong W, Chen H, Yang F, Lin S, Li C, Wang G. Inter-eye Differences in Ocular Biometric Parameters of Concomitant Exotropia. Front Med (Lausanne). 2021;8:724122. doi:10.3389/fmed.2021.724122 [PubMed: 35059408]
28. Thompson JR. The chi 2 test for data collected on eyes. Br J Ophthalmol. Feb 1993;77(2):115–7. doi:10.1136/bjo.77.2.115 [PubMed: 8435411]
29. Davis MD, Gangnon RE, Lee LY, et al. The Age-Related Eye Disease Study severity scale for age-related macular degeneration: AREDS Report No. 17. Archives of ophthalmology (Chicago, Ill : 1960). Nov 20. 1484–98:)11(123;05doi:10.1001/archopht.123.11.1484/10.1001archopht.123.11.1484.
30. Pai AS-I, Mitchell P, Rochtchina E, Iyengar S, Wang JJ. Complement Factor H and the Bilaterality of Age-Related Macular Degeneration: The Blue Mountains Eye Study. Archives of Ophthalmology. 2009;127(10):1339–1344. doi:10.1001/archophthalmol.2009.239 [PubMed: 19822851]
31. Barondes M, Pauleikhoff D, Chisholm IC, Minassian D, Bird AC. Bilaterality of drusen. Br J Ophthalmol. Mar 1990;74(3):180–2. doi:10.1136/bjo.74.3.180 [PubMed: 2322518]
32. Garcia Filho CA, Yehoshua Z, Gregori G, et al. Change in drusen volume as a novel clinical trial endpoint for the study of complement inhibition in age-related macular degeneration. Ophthalmic surgery, lasers & imaging retina. Jan-Feb 2014;45(1):18–31. doi:10.3928/23258160-20131217-01
33. Chavali VR, Diniz B, Huang J, Ying GS, Sadda SR, Stambolian D. Association of OCT derived drusen measurements with AMD associated-genotypic SNPs in Amish population. J Clin Med. 2015;4(2):304–317. doi:10.3390/jcm4020304 [PubMed: 25893111]
34. Hoffman GE, Schadt EE. variancePartition: interpreting drivers of variation in complex gene expression studies. BMC Bioinformatics. Nov 25 2016;17(1):483. doi:10.1186/s12859-016-1323-z [PubMed: 27884101]
35. Kersten E, Paun CC, Schellevis RL, et al. Systemic and ocular fluid compounds as potential biomarkers in age-related macular degeneration. Surv Ophthalmol. Jan - Feb 2018;63(1):9–39. doi:10.1016/j.survophthal.2017.05.003 [PubMed: 28522341]
36. Pietraszkiewicz A, van Asten F, Kwong A, et al. Association of Rare Predicted Loss-of-Function Variants in Cellular Pathways with Sub-Phenotypes in Age-Related Macular Degeneration. Ophthalmology. Mar 2018;125(3):398–406. doi:10.1016/j.ophtha.2017.10.027 [PubMed: 29224928]
37. Seddon JM, Rosner B. Validated Prediction Models for Macular Degeneration Progression and Predictors of Visual Acuity Loss Identify High-Risk Individuals. Am J Ophthalmol. Feb 2019;198:223–261. doi:10.1016/j.ajo.2018.10.022 [PubMed: 30389371]
38. van Asten F, Simmons M, Singhal A, et al. A Deep Phenotype Association Study Reveals Specific Phenotype Associations with Genetic Variants in Age-related Macular Degeneration: Age-Related Eye Disease Study 2 (AREDS2) Report No. 14. Ophthalmology. Apr 2018;125(4):559–568. doi:10.1016/j.ophtha.2017.09.023 [PubMed: 29096998]
39. Hammond CJ, Webster AR, Snieder H, Bird AC, Gilbert CE, Spector TD. Genetic influence on early age-related maculopathy: a twin study. Ophthalmology. Apr 2002;109(4):730–6. doi:10.1016/s0161-6420(01)01049-1/10.1016s0161-6420(01)01049-1. [PubMed: 11927430]
40. Sunness JS, Bressler NM, Tian Y, Alexander J, Applegate CA. Measuring geographic atrophy in advanced age-related macular degeneration. Invest Ophthalmol Vis Sci. Jul 1999;40(8):1761–9. [PubMed: 10393046]
41. Chang B, Yannuzzi LA, Ladas ID, Guyer DR, Slakter JS, Sorenson JA. Choroidal neovascularization in second eyes of patients with unilateral exudative age-related macular degeneration. Ophthalmology. Sep 1995;102(9):1380–6. doi:10.1016/s0161-6420(95)30860-3/10.1016s0161-6420(95)30860-3. [PubMed: 9097777]
42. Parikh R, Avery RL, Saroj N, Thompson D, Freund KB. Incidence of New Choroidal Neovascularization in Fellow Eyes of Patients With Age-Related Macular Degeneration Treated With Intravitreal Aflibercept or Ranibizumab. JAMA Ophthalmol. Jul 11 2019;doi:10.1001/jamaophthalmol.2019.1947

43. Strahlman ER, Fine SL, Hillis A. The second eye of patients with senile macular degeneration. Archives of ophthalmology (Chicago, Ill : 1960). Aug 1983;101(8):1191–3. doi:10.1001/archopht.1983.01040020193003/10.1001archopht.1983.01040020193003. [PubMed: 6882244]

44. Hibert ML, Chen YI, Ohringer N, et al. Altered Blood Flow in the Ophthalmic and Internal Carotid Arteries in Patients with Age-Related Macular Degeneration Measured Using Noncontrast MR Angiography at 7T. AJNR Am J Neuroradiol. Sep 2021;42(9):1653–1660. doi:10.3174/ajnr.A7187 [PubMed: 34210664]

45. Rosenfeld PJ, Trivizki O, Gregori G, Wang RK. An Update on the Hemodynamic Model of Age-Related Macular Degeneration. Am J Ophthalmol. Sep 9 2021;235:291–299. doi:10.1016/j.ajo.2021.08.015 [PubMed: 34509436]

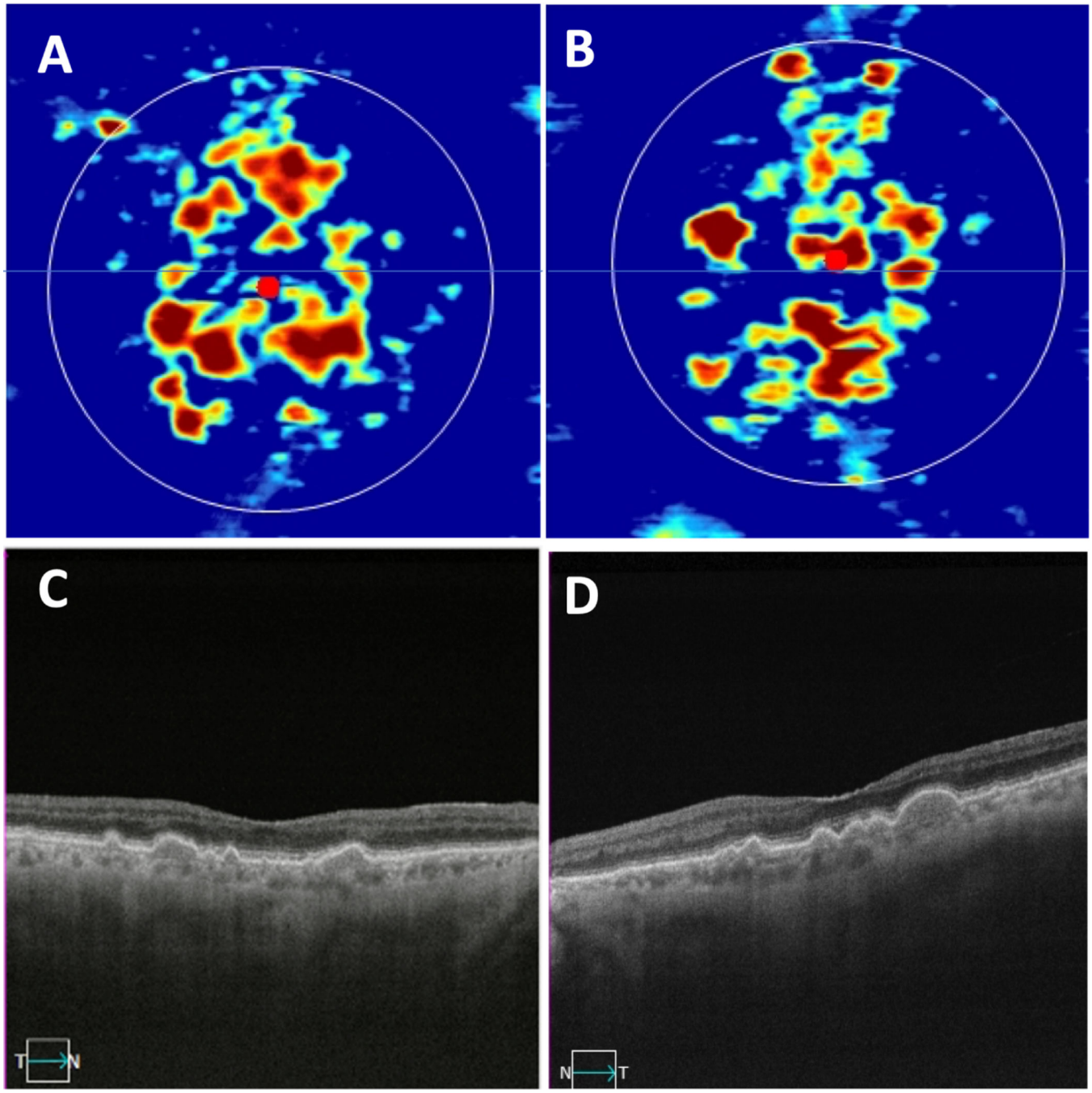

Figure 1.

Bilateral drusen-only eyes with non-exudative age-related macular degeneration. (A, B) Swept-source OCT drusen maps of the right and left eyes, respectively. (C,D) Central foveal B-scans showing drusen in the same right and left eyes shown in panels A and B.

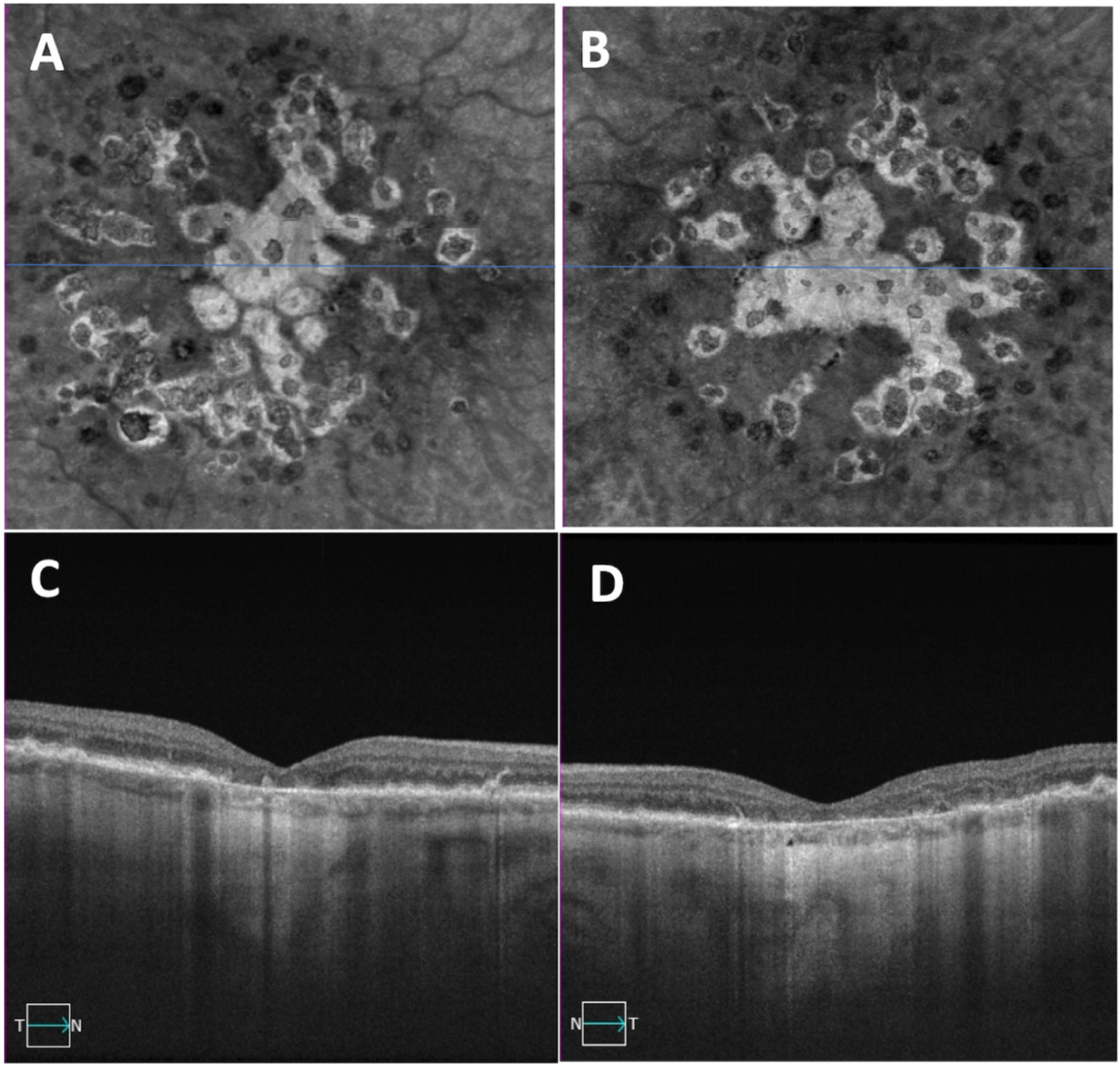

Figure 2.

Bilateral eyes with geographic atrophy (GA) secondary to non-exudative age-related macular degeneration. (A, B) *En face* swept-source OCT images derived from sub-RPE slabs showing hypertransmission defects corresponding to GA in both eyes. (C,D) Central foveal B-scans showing evidence of choroidal hypertransmission defects corresponding to the en face OCT images shown in panels A and B.

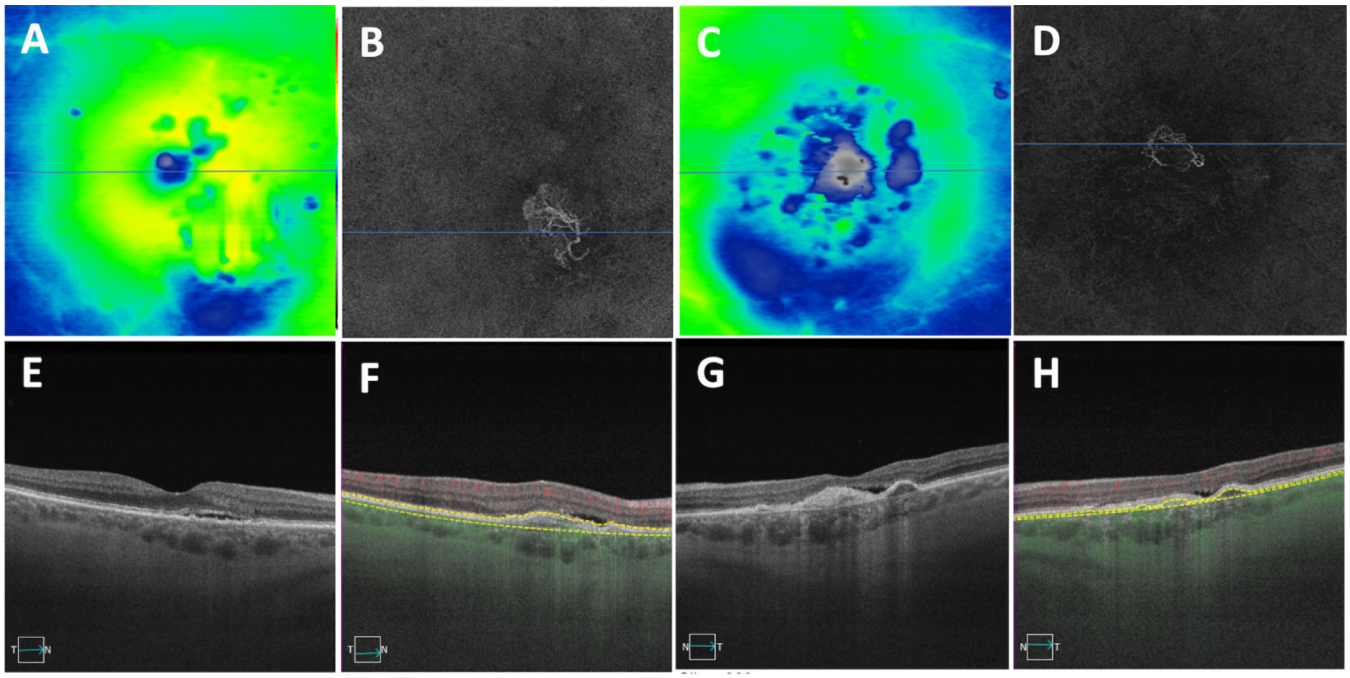

Figure 3.

Macular neovascularization (MNV) in both eyes secondary to exudative age-related macular degeneration. (A, C) Swept-source OCT (SS-OCT) thickness maps of the right and left eyes. (B,D), SS-OCT angiography (SS-OCTA) images showing *en face* slabs with segmentation boundaries from the retinal pigment epithelium (RPE) to Bruch's membrane depicting type 1 macular neovascularization. (E,G) Central foveal SS-OCT B-scans showing evidence of subretinal fluid in both eyes. (F,H) B-scans with segmentation boundaries and flow used to detect MNV on the corresponding *en face* images in panels B and D, respectively.

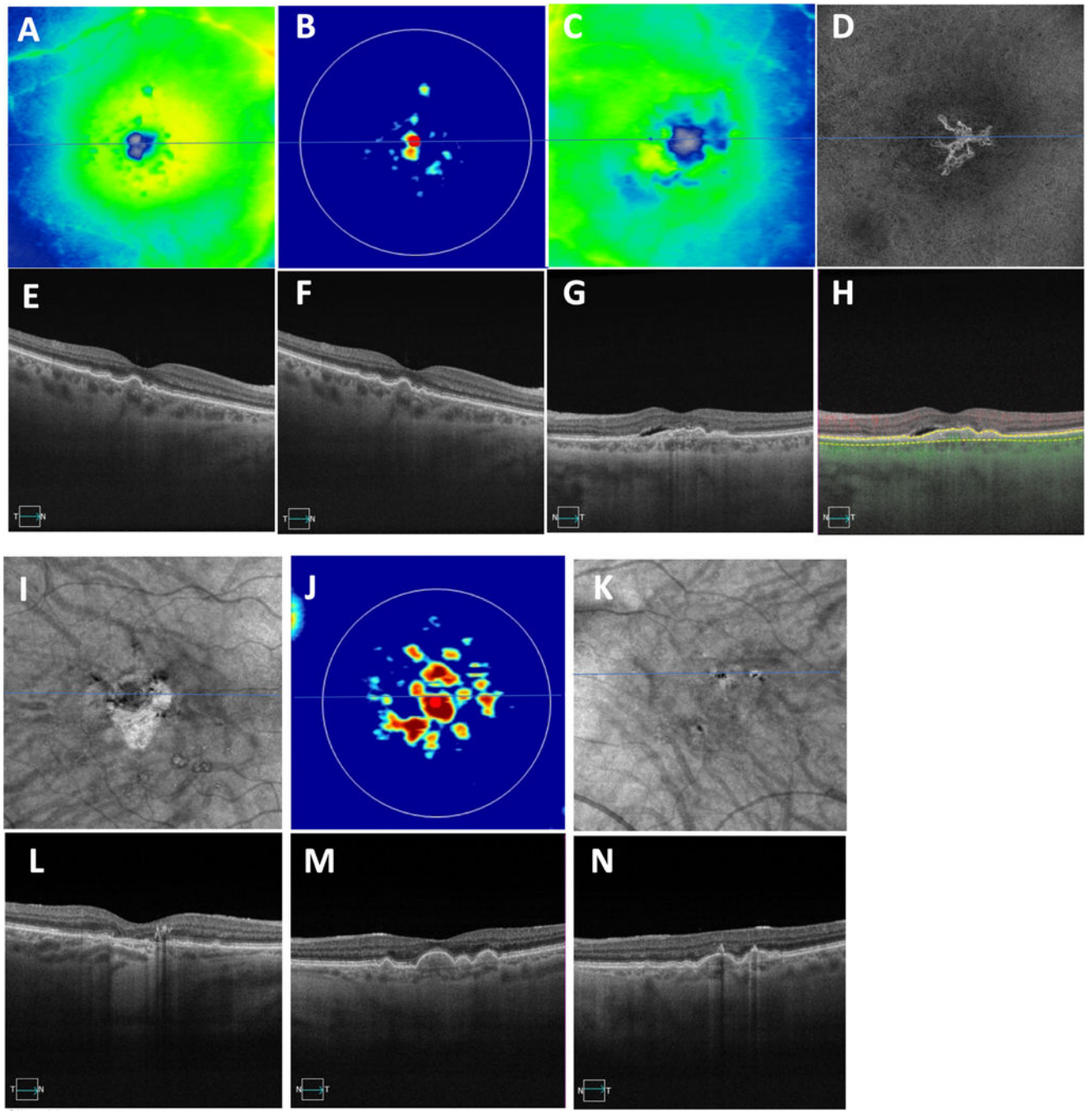

Figure 4.

Two cases showing asymmetric presentation of drusen and late AMD in the fellow eye. (A-H) First case of drusen in the right eye and macular neovascularization (MNV) in the left eye. (A,C) Thickness maps with (E-G) showing central foveal SS-OCT B-scans, (G) showing evidence of subretinal fluid, (B) showing swept-source OCT drusen map of the right eye, (D, H) showing *en face* slabs with segmentation boundaries from the retinal pigment epithelium (RPE) to Bruch's membrane depicting type 1 macular neovascularization, (H) showing B-scans with segmentation boundaries and flow used

to detect MNV on the corresponding en face images in (D). (I-N) The second case showing GA in the right eye and drusen in the left eye. (I,K) *En Face* swept-source OCT images derived from sub-RPE slabs showing hypertransmission defects corresponding to GA in the right eye with no defects in the left eye. (L, N) Central foveal B-scans showing evidence of choroidal hypertransmission defects corresponding to the en face OCT images shown in (I) and hypo-transmission defects (black spots) in the left eye due to overlying hyperpigmentation. (J) Swept-source OCT drusen map of the left eye with (M) corresponding to the central foveal SS-OCT B-scan

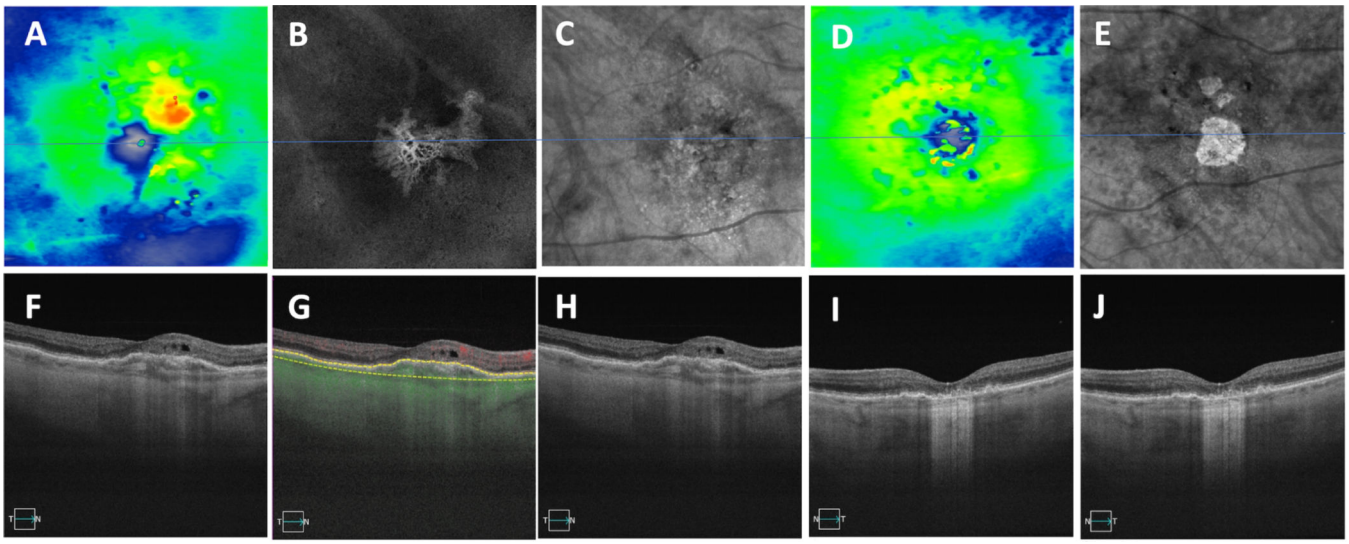

Figure 5.

A case showing asymmetric presentation of late AMD in both eyes with macular neovascularization (MNV) in the right eye and geographic atrophy (GA) in the left eye. (A,D) Thickness maps with (F,I) showing central foveal SS-OCT B-scan, (F) showing evidence of intraretinal fluid, (B) showing an *en face* slab with segmentation boundaries from the retinal pigment epithelium (RPE) to Bruch's membrane depicting the type 1 macular neovascularization, (G) showing B-scans with segmentation boundaries and flow used to detect MNV on the corresponding en face images in panel D. (C,E) *En Face* swept-source OCT images derived from sub-RPE slabs showing hypertransmission defects corresponding to GA in the left eye with no defects in the right eye, (H,J) showing central foveal B-scans with evidence of choroidal hypertransmission defects corresponding to the *en face* OCT images shown in (E) with no clear defect in the right eye (C).

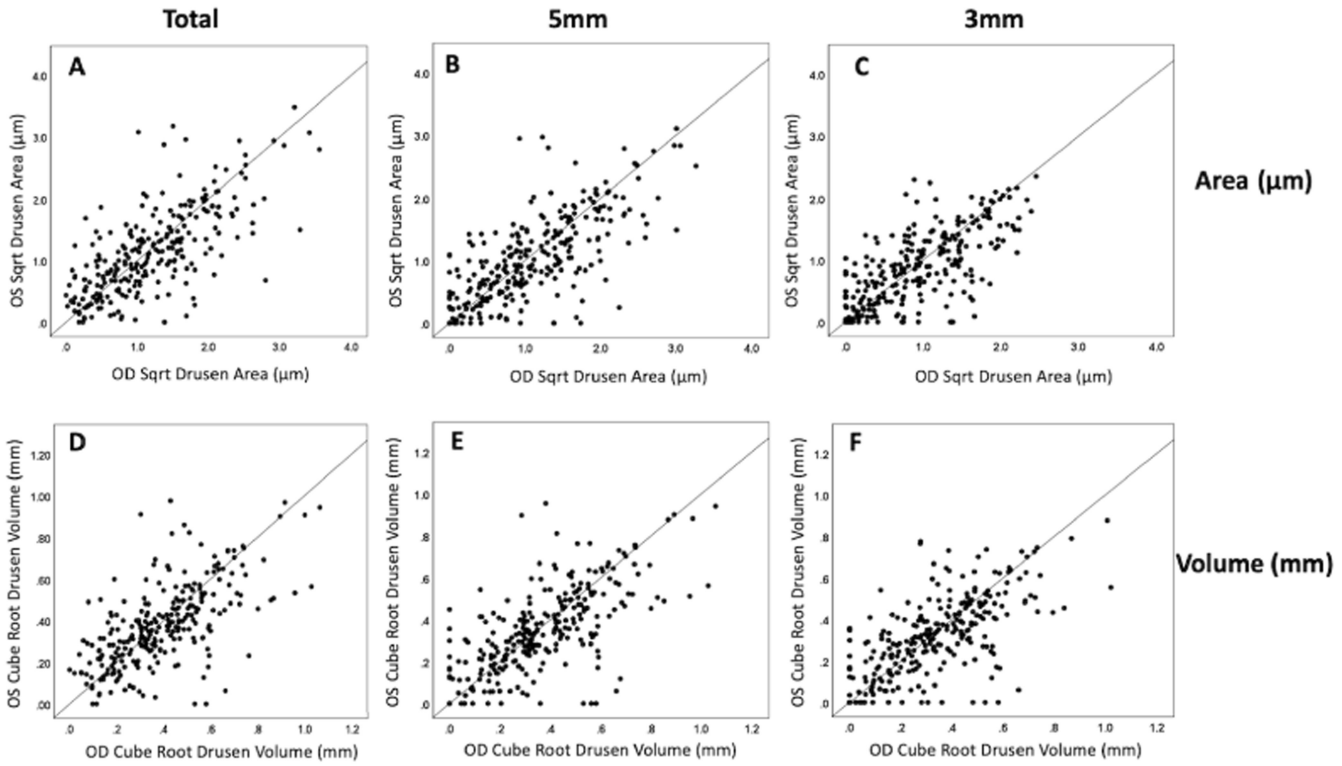

Figure 6.

Scatter plot comparisons of the drusen area using a square-root transformation and drusen volume using a cube-root transformation. (A, B, C) Square-root of drusen areas within the total scan area and within foveal-centered circles with diameters of 3 mm and 5 mm. (D, E, F) Cube-root of drusen volumes within the total scan area and within foveal-centered circles with diameters of 3 mm and 5 mm. All $p>0.05$. (OD=right eye, OS=left eye).

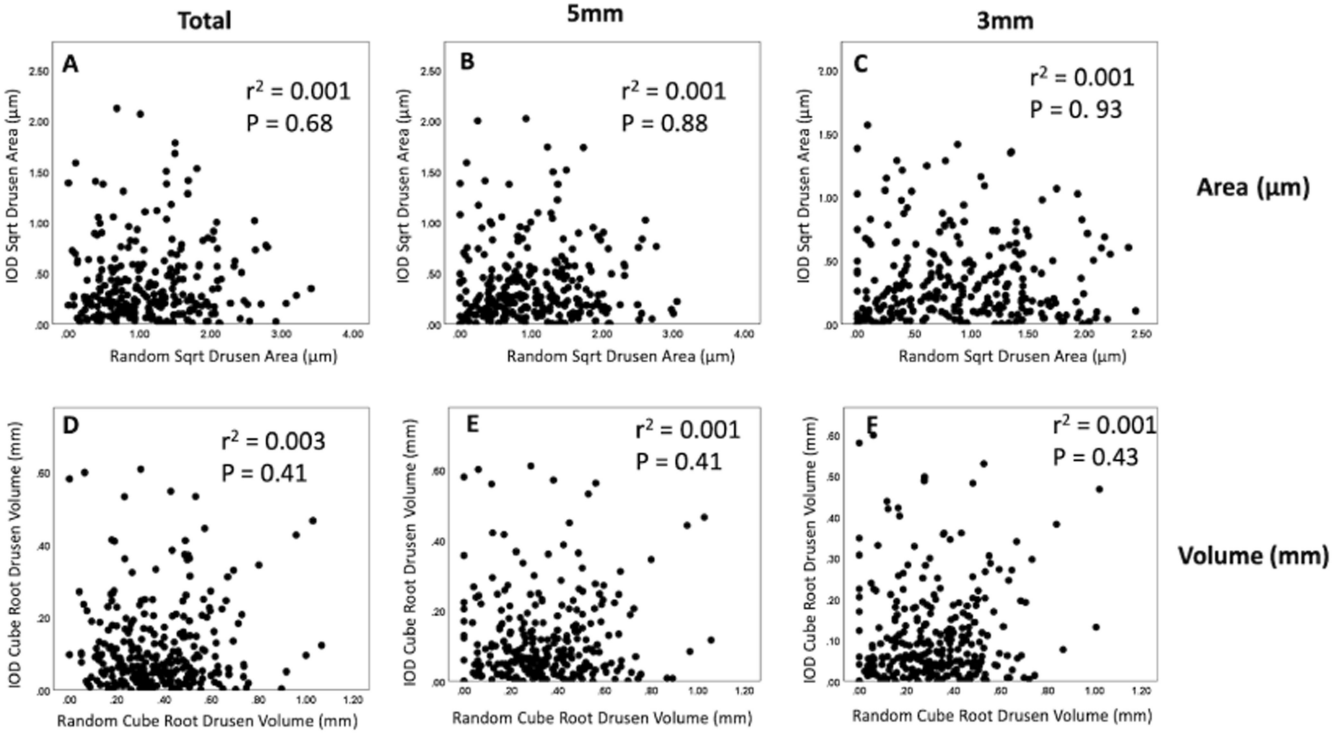

Figure 7.

Scatter plot correlations between the square-root of drusen area and the cube-root of drusen measurements versus their intraocular differences. (A, B, C) Square-root of drusen areas within the total scan area and within foveal-centered circles with diameters of 3 mm and 5 mm. (D, E, F) Cube-root of drusen volumes within the total scan area and within foveal-centered circles with diameters of 3 mm and 5 mm. No associations were found using linear, quadratic, cubic, growth, or exponential tests. (r squared values<0.03). Right or left eyes were chosen at random to be index eye.

Table 1.

Percentage agreement of disease gradings between randomly selected index eyes (IE) and fellow eyes (FE).

Disease Gradings % (n)	FE Dry disease – Drusen	FE Dry disease – GA	FE Wet disease – MNV	FE Mixed disease (MNV and GA)
IE Dry Disease – Drusen	20% (265)	3% (33)	14% (181)	0% (3)
IE Dry Disease – GA	2% (29)	11% (148)	5% (62)	0% (5)
IE Wet disease – MNV	15% (199)	5% (69)	22% (287)	1% (11)
IE Mixed disease (MNV and GA)	0% (3)	0% (3)	1% (6)	1% (6)

IE: index eyes; FE: fellow eyes; GA: geographic atrophy; MNV: macular neovascularization

Table 2.

Interocular Symmetry Differences Between Eyes

Type	Scan Size	Mean (SD)	Median	Percent of all interocular differences		ICC
				50% [LL, UL]	95% [LL, UL]	
Cube root drusen volume	Total	0.02 (0.17)	0.05	[−0.06, 0.09]	[−0.37, 0.43]	0.64
	5mm	0.02 (0.17)	0.03	[−0.06, 0.09]	[−0.32, 0.45]	0.66
	3mm	0.02 (0.17)	0.03	[−0.06, 0. 09]	[−0.34, 0.43]	0.65
Square root drusen area	Total	0.06 (0.55)	0.05	[−0.23, 0.33]	[−1.17, 1.38]	0.70
	5mm	0.06 (0.54)	0.03	[−0.23, 0.32]	[−1.05, 1.38]	0.71
	3mm	0.05 (0.48)	0.03	[−0.21, 0.30]	[−0.99, 1.22]	0.70

SD: Standart Deviation; 50% LL: Lower Limit = 25^{th}%tile; 50^{th}%tile UL: Upper Limit = 75%tile; 95% LL: Lower Limit = 2.5^{th}%tile; 95^{th}%tile UL: Upper Limit = 97.5%tile; ICC Intraclass Correlation Coefficient

Table 3.

Difference between eyes in total drusen area and volume for patients with only bilateral drusen by quintiles

Quintiles of SQRT drusen area, both eyes averaged	**Mean (SD) Absolute value interocular difference in SQRT drusen area**
≤ 0.54	0.27 (0.22)
>0.54 – 0.91	0.40 (0.36)
>0.91 – 1.26	0.43 (0.40)
>1.26 – 1.74	0.43 (0.49)
≥ 1.74	0.40 (0.38)
Quintiles of CBRT drusen volume, both eyes averaged	**Mean (SD) Absolute value interocular difference in CBRT drusen volume**
≤0.22	0.09 (0.09)
>0.22 – 0.32	0.12 (0.13)
>0.32 – 0.41	0.11 (0.13)
>0.41 – 0.53	0.12 (0.11)
>0.53 – 1.00	0.14 (0.13)

P > 0.05 for all quintiles; SD standard deviation; SQRT: square root; CBRT: cube root